OPEN

Molecular Psychiatry (2014) 19, 937–946

www.nature.com/mp

ORIGINAL ARTICLE

Chronic γ-secretase inhibition reduces amyloid plaque-associated instability of pre- and postsynaptic structures

S Liebscher[1,2], RM Page[2], K Käfer[1], E Winkler[2], K Quinn[3], E Goldbach[3], EF Brigham[3], D Quincy[3], GS Basi[3], DB Schenk[4], H Steiner[2,5], T Bonhoeffer[1], C Haass[2,5,6], M Meyer-Luehmann[2,7,8] and M Hübener[1,7]

The loss of synapses is a strong histological correlate of the cognitive decline in Alzheimer's disease (AD). Amyloid β − peptide (Aβ), a cleavage product of the amyloid precursor protein (APP), exerts detrimental effects on synapses, a process thought to be causally related to the cognitive deficits in AD. Here, we used *in vivo* two-photon microscopy to characterize the dynamics of axonal boutons and dendritic spines in APP/Presenilin 1 ($APP_{swe}/PS1_{L166P}$)–green fluorescent protein (GFP) transgenic mice. Time-lapse imaging over 4 weeks revealed a pronounced, concerted instability of pre- and postsynaptic structures within the vicinity of amyloid plaques. Treatment with a novel sulfonamide-type γ-secretase inhibitor (GSI) attenuated the formation and growth of new plaques and, most importantly, led to a normalization of the enhanced dynamics of synaptic structures close to plaques. GSI treatment did neither affect spines and boutons distant from plaques in amyloid precursor protein/presenilin 1-GFP (APPPS1-GFP) nor those in GFP-control mice, suggesting no obvious neuropathological side effects of the drug.

Molecular Psychiatry (2014) **19,** 937–946; doi:10.1038/mp.2013.122; published online 24 September 2013

Keywords: Alzheimer's disease; APP-transgenic mice; gamma secretase inhibitor; two-photon imaging; dendritic spines; axonal boutons

INTRODUCTION

Alzheimer's disease (AD) is characterized by a progressive decline of memory function and cognition. Hallmarks of AD pathology are extracellular aggregates of the amyloid β-peptide (Aβ), so-called amyloid plaques, and neurofibrillary tangles, which represent intraneuronal aggregates of hyperphosphorylated tau protein. The strongest correlate of the cognitive decline seen in AD, however, is the loss of synapses.[1–3] Moreover, there is mounting evidence for synaptic dysfunction and failure in AD both *in vitro* and *in vivo* (reviewed by Koffie *et al.*[4] and Selkoe[5]). Oligomeric Aβ, as one of the key factors in AD,[4–7] is known to colocalize with dendritic spines—the main sites of synaptic input to excitatory pyramidal neurons—potentially binding to molecular components of the postsynapse,[8–10] and thereby exhibiting deleterious effects on dendritic spines.[4,7,11] This negative impact of Aβ on dendritic spines is most pronounced in close vicinity to amyloid plaques, causing an impairment of spine stability, which is thought to result in the loss of spines[12–15] and ultimately synaptic connections.

Previous *in vivo* imaging studies have largely focused on the impact of amyloid plaques on dendritic spines,[15,16] whereas not much is known about the presynaptic side, namely axonal boutons, *in vivo*. Histological studies, mostly using presynaptic markers, reported an overall decrease in synaptic density in AD patients,[1,2] whereas only a local reduction of presynaptic marker density close to plaques was observed in amyloid precursor protein (APP) transgenic mice.[17–19] Given the described effect of Aβ on the dynamics and density of dendritic spines, we hypothesized that these amyloid plaque-associated postsynaptic alterations should be paralleled by changes of the presynaptic compartment, either directly caused by the plaque itself or secondary to changes of spines.

In the current study, we thus used *in vivo* two-photon imaging to follow dendritic spines and axonal boutons over the course of several weeks in wild-type (WT) and amyloid precursor protein/presenilin 1 (APPPS1) mice. We found an enhanced instability of both, pre- and postsynaptic structures, seen, for example, as a higher turnover rate and a lower survival fraction, limited to the immediate vicinity of plaques.

We then investigated whether these pathologically increased synaptic dynamics can be reduced or halted by treatment targeting Aβ generation. As Aβ is liberated upon sequential cleavage of APP by the β- and γ-secretase,[6,20] pharmacological inhibition of γ-secretase represents one way to interfere with Aβ generation. Although γ-secretase inhibitors (GSIs) have been shown to efficiently lower Aβ levels in the central nervous system (CNS) and reduce amyloid plaque load in animal models of the disease,[21,22] little is known about their potential to prevent plaque-associated synapse pathology.

We thus applied the novel, selective GSI (ELN594) daily for 4 weeks, and monitored plaque progression and associated dendritic spine and axonal bouton pathology in APPPS1 mice. GSI treatment reduced *de novo* plaque formation after the first week of treatment, slowed down the growth of these newly deposited plaques and, importantly, stabilized spines near plaques by lowering their turnover rate and increasing their survival

[1]Max Planck Institute of Neurobiology, Martinsried, Germany; [2]Department of Biochemistry, Adolf-Butenandt-Institute, Ludwig-Maximilians-University, Munich, Germany; [3]Élan Pharmaceuticals, Inc., Cambridge, MA, USA; [4]Prothena Biosciences, South San Francisco, CA, USA; [5]German Center for Neurodegenerative Diseases (DZNE), Munich, Germany and [6]Munich Cluster for Systems Neurology (SyNergy), Munich, Germany. Correspondence: Professor M Hübener, Max Planck Institute of Neurobiology, Am Klopferspitz 18, D-82152 Martinsried, Germany or Professor M Meyer-Luehmann, Neurocenter, Department of Neurology, University of Freiburg, Breisacher Str. 64, Freiburg, D-79106, Germany.
E-mail: mark@neuro.mpg.de or melanie.meyer-luehmann@uniklinik-freiburg.de
[7]These authors contributed equally to this work.
[8]Present address: Neurocenter, Department of Neurology, University of Freiburg, Breisacher Str. 64, D-79106 Freiburg, Germany.
Received 28 March 2013; revised 6 August 2013; accepted 8 August 2013; published online 24 September 2013

fraction. Likewise, GSI treatment normalized the survival fraction of boutons near plaques. Spines and boutons further away from plaques in APPPS1 mice and in WT mice were not affected by the GSI treatment.

MATERIALS AND METHODS

Animals for *in vivo* imaging experiments

For chronic *in vivo* imaging experiments, APPPS1$^{+/-}$ transgenic mice (co-expressing APP containing the Swedish double-mutation KM670/671NL and PS1 containing the L166P mutation under the Thy-1 promoter)[23] were crossbred with green fluorescent protein (GFP)-M$^{+/+}$ transgenic mice (expressing EGFP under the Thy-1 promoter, causing sparse labeling of mainly cortical layer V pyramidal neurons).[24] Animals were kept under a 12/12-h light–dark cycle with food and water *ad libitum* and housed individually on standard cage bedding, without additional nesting material. All animal procedures followed a protocol approved by the local authorities (Regierung von Oberbayern). For imaging experiments, only male mice were used.

Drug administration

Male mice were treated with ELN594 (Elan Pharmaceuticals, South San Francisco, CA, USA (see synthesis approach[25])) at the age of 3–4 months. The drug, dissolved in 2% methyl cellulose and 0.5% Tween20, was administered daily for four subsequent weeks via oral gavage at 30 mg kg^{-1}. All control mice received vehicle solution (2% methyl cellulose and 0.5% Tween20) only. Treatment started immediately after the first imaging session.

In vivo imaging

In brief, 4 weeks after implantation of a cranial window spanning both hemispheres (coordinates of craniotomy: Bregma +1.5– −3.5 mm, 3 mm lateral from midline on each side) the apical tufts of GFP-expressing layer V pyramidal neurons and axonal boutons of layer II/III/V neurons, as well as amyloid plaques were repeatedly imaged at 7-day intervals. Amyloid plaques were stained by intraperitoneal injection of the dye Methoxy-XO4 (Neuroptix Corporation) 24 h prior to every imaging session.

Details on drug characterization, cranial window surgery, imaging, data analysis and statistics are provided in Supplementary Materials and Methods.

RESULTS

In order to characterize the impact of amyloid plaque pathology on the dynamics of synaptic structures *in vivo,* we performed longitudinal *in vivo* two-photon imaging in male WT and APPPS1 mice (Supplementary Figure S1). We then assessed whether pharmacological interference with Aβ generation exerts beneficial effects on plaque-associated synaptic pathology in APPPS1 mice. To this end, we administered the selective GSI, ELN594 (see Supplementary Results), daily (30 mg kg^{-1}), for 4 consecutive weeks to WT and APPPS1 mice at the ages of 3–4 months and monitored amyloid pathology, dendritic spines and axonal boutons *in vivo* throughout the treatment period.

Amyloid plaque-associated spine pathology

As there is accumulating evidence that plaques cause neuritic and spine pathology predominantly within 50 μm distance to plaques,[12,14–16,26,27] we analyzed dendritic spines on apical tufts of layer V pyramidal neurons in WT (Figure 1a) and APPPS1 mice in the immediate vicinity of plaques (<50 μm, 'near'; Figure 1b) and further away (>50 μm, 'distant'). As described before[13,15,16] (for review see Liebscher and Meyer-Luehmann[28]), we found that dendritic stretches within the immediate vicinity of amyloid plaques exhibited a lower spine density (average over all time points 0.22 ± 0.017 μm^{-1}) compared with stretches further away from plaques in APPPS1 (0.28 ± 0.013 μm^{-1}) and WT mice (0.29 ± 0.017 μm^{-1}, Figure 1c). A more detailed analysis revealed that spine density was significantly reduced up to 15 μm from the plaque border compared with the spine density of WT vehicle-treated mice[13,15] (Supplementary Figure S2a) and that spine density was positively correlated with plaque distance up to 50 μm away from the plaque border (Pearson's correlation coefficient $r = 0.23$, $P = 0.01$). The drop in spine density near plaques did not depend on plaque size ($r = -0.05$, $P = 0.56$; Supplementary Figure S2a).

Determining spine density alone is insufficient to capture all aspects of potential (pathological) spine alterations, as they are dynamic structures, which are lost and gained at a certain rate, even under baseline conditions.[29–32] We hence determined the spine survival fraction and turnover rate and classified spines, according to their lifetime, as persistent or transient (Figure 1e). Spines close to plaques are less stable, which is reflected in a lower survival fraction (Figure 1d), a lower fraction of persistent spines compared with spines distant from plaques and in WT mice (Figure 1f) and, accordingly, a higher fraction of transient spines (Figure 1f). The high turnover rate of spines near plaques (Figure 1g) resulted from both an increased elimination (Figure 1h) and formation rate (Figure 1i). The elevated spine turnover did neither depend on plaque proximity within a 50 μm radius to the plaque border ($r = 0.04$, $P = 0.79$) nor on plaque size ($r = -0.09$, $P = 0.51$, Supplementary Figure S2b).

There was no significant difference between spines in WT mice and spines further away from plaques in APPPS1 mice for any of the spine parameters analyzed. A more detailed analysis, however, revealed a negative correlation between turnover rate and spine density in WT mice in line with a previous publication.[30] Interestingly, this correlation was positive for dendrites further away from plaques in APPPS1 mice (WT: $r = -0.52$, $P = 0.039$; APPPS1: $r = 0.47$, $P = 0.025$; Supplementary Figure S3a). This difference was largely due to dendritic stretches with a low spine density (0.15–0.26 μm^{-1}), which exhibited a significantly lower spine turnover rate in APPPS1 mice (Supplementary Figure 3b). The absolute density of gained spines was independent of the total spine density in WT mice ($r = 0.011$, $P = 0.97$, Supplementary Figure 3c). In contrast, in APPPS1 mice, dendrites distant from plaques exhibited a significant positive correlation between the density of gained spines and total spine density ($r = 0.73$, $P < 0.001$, Supplementary Figure 3c). Again low-density dendrites (≤0.26 μm^{-1}) in APPPS1 mice had a significantly lower density of newly formed spines in comparison with WT mice (Supplementary Figure 3d). These data indicate a plaque-independent effect on spine dynamics in APPPS1-transgenic mice, which mainly affects dendritic stretches with a low spine density. We did not observe a significant correlation between spine density and turnover rate for spines close to plaques ($r = -0.47$, $P = 0.12$).

Amyloid plaque-associated axonal bouton pathology

Not much is known about the dynamics of plaque-associated presynaptic structures. We therefore analyzed axonal boutons located within the same imaged volumes as the above described dendrites. We took advantage of the fact that bouton dynamics were described in detail for the GFP-M mouse line in a recent publication.[33] Based on this study and judged by bouton size as well as the number and length of axonal branches, the majority of axons investigated are putatively originating from layer II/III/V cells (Figures 2a and b). In addition to en passant boutons, which represented the majority of boutons, terminaux boutons were included in the analyses, as their fraction was low and did not differ significantly between groups (fraction terminaux boutons: WT 0.04 ± 0.065, APP distant 0.09 ± 0.12, APP near 0.076 ± 0.1, Kruskal–Wallis, $P = 0.45$).

We did not find a significant difference in bouton density between WT and APPPS1 mice (WT 0.12 ± 0.01 μm^{-1}, APP distant 0.12 ± 0.01 μm^{-1}, APP near 0.13 ± 0.013 μm^{-1}, Figure 2c). Furthermore, on axonal stretches close to plaques, the

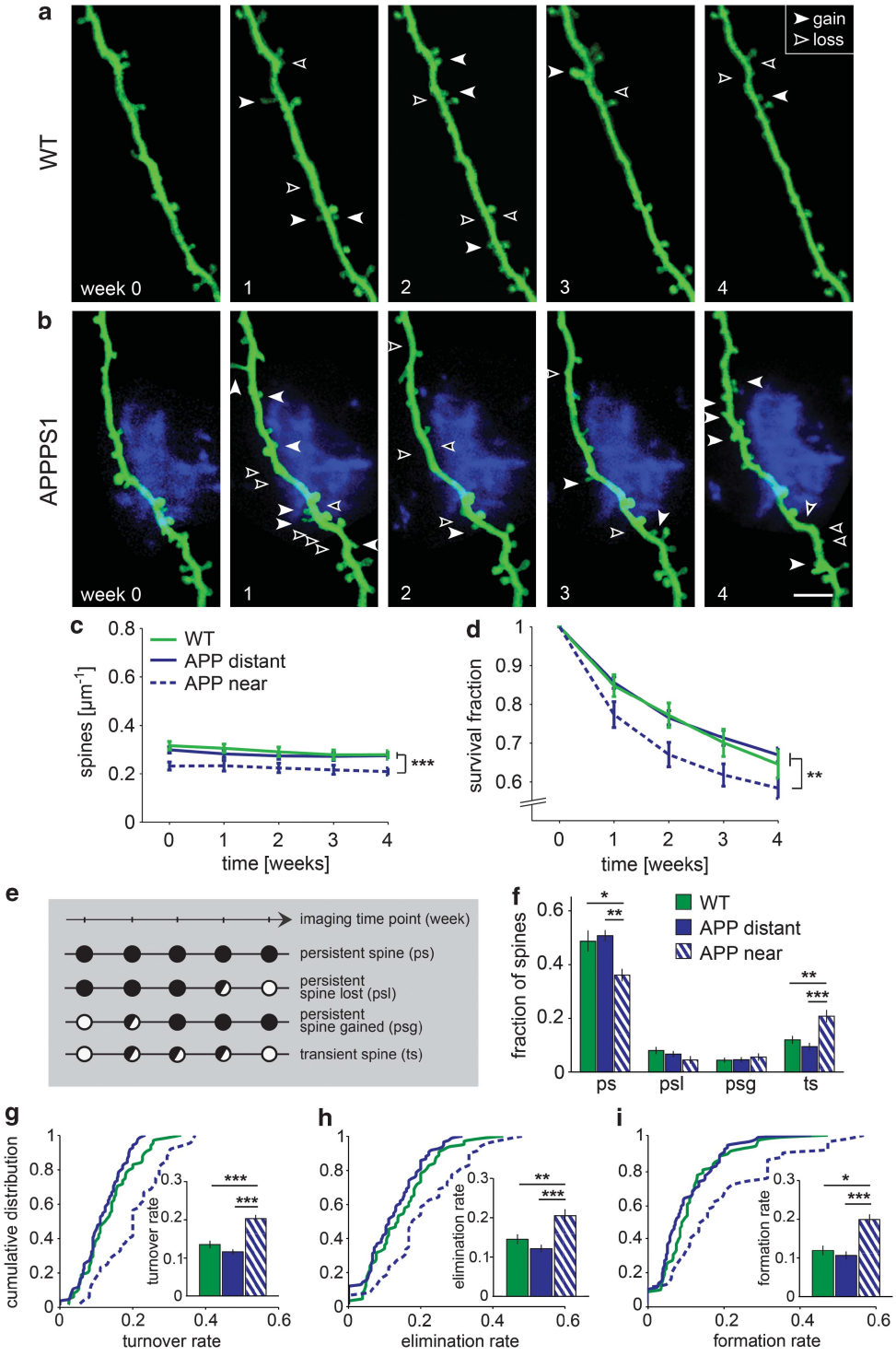

Figure 1. Amyloid plaque-associated dendritic spine alterations. (**a** and **b**) Representative examples of apical dendritic stretches of layer V pyramidal neurons repeatedly imaged within layer I over the course of 4 weeks in wild-type (WT) and amyloid precursor protein/presenilin 1 (APPPS1) mice (shown are maximum projections). Note that the actual position of the dendritic stretch in panel **b** is just above the plaque, with the dendrite not passing through it. Open arrowhead: spine lost, filled arrowhead: spine gained. (**c**) Spine density is significantly lower in the vicinity of plaques in APPPS1 mice, compared with dendrites further away from plaques and WT mice, respectively (repeated measures analysis of variance (ANOVA); $P<0.001$ and $P<0.001$). (**d**) Survival fraction of spines near plaques is significantly decreased (repeated measures ANOVA, $P<0.001$). (**e**) Classification of spines with respect to their lifetime. Filled circles denote the presence of a spine at the respective time point, open circles correspond to the absence of a spine and half-filled circles denote a spine being either present or absent at the respective time point. (**f**) Dendrites near plaques have fewer persistent (one-way ANOVA, $P<0.01$ and $P<0.05$) and more transient spines compared with spines distant from plaques and in WT mice (one-way ANOVA, $P<0.001$ and $P<0.01$). (**g**) Spine turnover rates near plaques are significantly elevated compared with spines further away from plaques and WT mice, respectively (one-way ANOVA, $P<0.001$). (**h** and **i**) Increased turnover results from higher (**h**) elimination (one-way ANOVA, $P<0.001$ and $P<0.01$) and (**i**) formation rates (Kruskal–Wallis, $P<0.001$ and $P<0.05$). Data in panels **g**–**i** are average values over all imaging time points. WT: $n=16$ dendrites (four mice); APP distant: $n=21$ dendrites (five mice); APP near: $n=12$ dendrites (five mice). Values are mean ± s.e.m., scale bar 5 µm (**b**), $*P<0.05$, $**P<0.01$, $***P<0.001$.

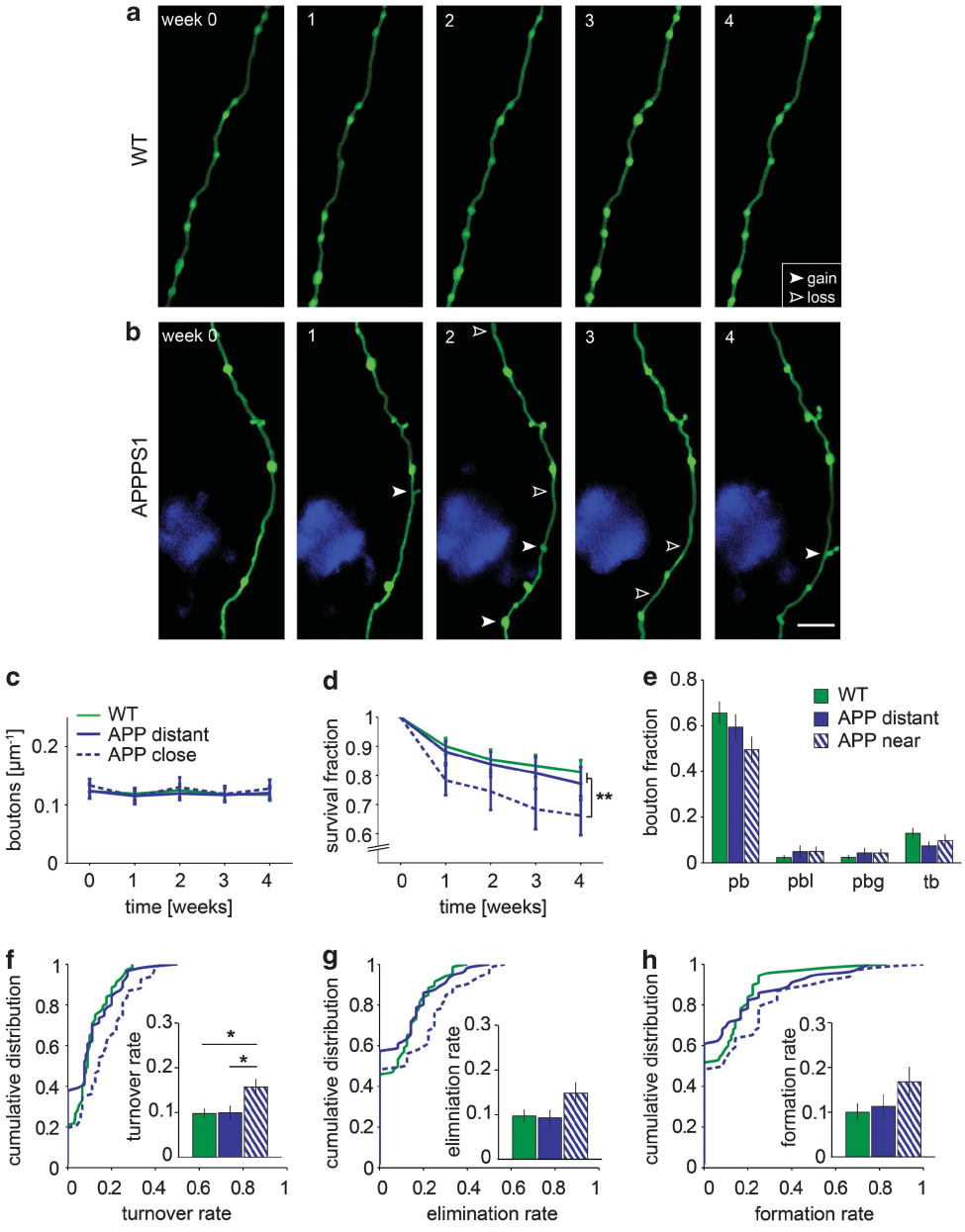

Figure 2. Bouton dynamics in wild-type (WT) and amyloid precursor protein/presenilin 1 (APPPS1) mice. (**a** and **b**) Examples of axonal stretches in (**a**) WT and (**b**) APPPS1 mice over the 4-week-imaging period are shown as maximum projections. Boutons lost from one time point to the next are marked with open arrowheads, boutons gained with filled arrowheads. (**c**) Bouton density is not different between axons near plaques, further away from plaques or in WT mice (repeated measures ANOVA, $P = 0.93$). (**d**) Boutons near plaques exhibit a lower survival fraction (repeated measures ANOVA, $P < 0.01$). (**e**) Bouton lifetime categories (see Figure 1e) do not differ significantly among groups (fraction persistent boutons: one-way ANOVA, $P = 0.12$, fraction transient: Kruskal–Wallis $P = 0.31$, fraction persistent lost: Kruskal–Wallis $P = 0.63$, fraction persistent gained: Kruskal–Wallis $P = 0.61$). (**f**) Turnover rate is increased on boutons close to plaques (Kruskal–Wallis, $P < 0.05$). Separate analysis of (**g**) elimination and (**h**) formation rate showed the same trend but did not reach significance (Kruskal–Wallis, $P = 0.23$ and $P = 0.24$). WT: $n = 17$ axons (four mice); APP distant: $n = 14$ axons (four mice); APP near: $n = 13$ axons (four mice). Values are mean ± s.e.m., scale bar 10 µm (**b**), $^{*}P < 0.05$, $^{**}P < 0.01$.

inter-bouton distance did also not depend on plaque proximity (Supplementary Figure S4). However, similar to our data on dendritic spines near plaques, the survival fraction of boutons near plaques was decreased compared with boutons further away from plaques and in WT mice (Figure 2d). Analysis of boutons with different lifetimes did not yield a significant difference between axons in APPPS1 and WT mice (Figure 2e). However, boutons near plaques exhibited a higher turnover rate compared with boutons further away from plaques and boutons in WT mice (Figure 2f). Separate analyses of elimination and formation rate showed the same trend but did not reach significance (Figures 2g and h). Overall, boutons appeared less dynamic than spines on apical tufts of layer V neurons, corroborating earlier reports.[30,33] Newly formed spines have been shown to preferentially target large multisynaptic boutons,[34] which could account for the observed difference.

Apart from the above mentioned changes in bouton dynamics, we occasionally observed the emergence of axonal dystrophies, axonal breakage and axonal sprouting within the peri-plaque region (Supplementary Figure S5). These structural alterations

occurred only rarely in APPPS1-GFP mice, probably attributable to the young age of 3–4 months and the sparse labeling of neurons in the GFP-M mouse line.

Initial reduction in *de novo* plaque deposition by GSI treatment

We next investigated whether the enhanced dynamics of synaptic structures near amyloid plaques can be halted by Aβ-targeting treatment. For this purpose, we tested the sulfonamide-type GSI ELN594 both in WT and APPPS1 mice.

ELN594 is an orally available, CNS penetrant and highly potent GSI (see Supplementary Results, Supplementary Figures S6a–c). As PS1 mutations of familial AD, such as the aggressive PS1L166P mutation[35] present in the mouse model used here, are known to be less sensitive to GSIs,[36] we first tested the effect of a single dose of ELN594 (30 mg kg^{-1}) on APP C-terminal fragments as well as Aβ40 and Aβ42 levels in brains of APPPS1-GFP mice 24 h after drug application. The GSI efficiently inhibited γ-secretase as shown by the pronounced accumulation of APP C-terminal fragments in the western blot analysis (219% compared with vehicle-treated animals, Figures 3a and b). In accordance with the observed increase in APP C-terminal fragment levels, we found that soluble Aβ40 and Aβ42 levels were significantly decreased by 66% and 59%, respectively, upon GSI application, indicating that GSI treatment efficiently lowers Aβ levels in the APPPS1 mouse model (Figure 3c).

We next analyzed the potential of the GSI to interfere with *de novo* deposition of plaques using repeated two-photon imaging (Figures 3d and e). We found that ELN594 affected plaque formation, manifested as a drop in the number and size of newly deposited plaques in GSI-treated APPPS1 mice compared with vehicle-treated mice after the first week of GSI treatment (Figures 3f and g). The observed decrease in newly formed plaques after 1 week of treatment ceased over the course of the experiment, and a general decline in the occurrence of new plaques was seen in both GSI-treated and control mice, which might reflect the age dependency of plaque deposition (Figure 3f). However, plaques newly formed within the first week of treatment grew significantly slower in GSI compared with vehicle-treated mice, indicating a sustained effect of the GSI throughout the treatment period (Figure 3h).

Effect of GSI treatment on plaque-associated spine and bouton alterations

We applied the GSI to APPPS1 mice daily for 4 consecutive weeks. WT mice were treated in addition in order to test for potential adverse effects of the treatment that have been described in a previous publication for unselective GSIs of a different structural class.[37] GSI treatment had neither an effect on spine density in APPPS1 (Figures 4a and b) nor on those in WT mice (Supplementary Figure S7a) over the course of the 4-week treatment period.

Importantly, GSI treatment counteracted the plaque-associated changes in spine dynamics. More specifically, in GSI-treated mice we found a higher spine survival fraction near plaques (Figure 4c), a higher fraction of persistent spines (Figure 4d) and accordingly a lower fraction of transient spines (Figure 4d) compared with spines near plaques in vehicle-treated mice. The pathologically enhanced elimination and formation rates of spines near plaques in vehicle-treated mice were reduced by the GSI to levels found on dendrites further away from plaques (Figures 4e–g). Note that presented here are average values over all time points, as spine dynamics were consistently elevated throughout the treatment period (see Supplementary Figures S8a–c).

As the density of spines within a radius of 50 μm to the plaque edge correlates well with the effective plaque distance (Supplementary Figure S2a), we investigated whether GSI treatment affects spines in a distance-dependent manner. Whereas the GSI had no effect on spine density near plaques at any given distance between 0 and 50 μm, the turnover rate was significantly reduced for spines that were >15 μm (yet <50 μm) away from the plaque border (Supplementary Figures S9a–d).

In addition to alterations in synapse number and turnover, pathology might also be reflected in changes to the strength of a synapse, which is known to correlate well with spine size.[34,38,39] We hence determined integrated spine brightness as a measure for spine size.[31] In line with a previous report,[40] the overall distribution of spine sizes resembled a log-normal distribution, both for spines close to plaques in APP and WT mice (Supplementary Figures S10a–c). Average spine size as well as spine-size distribution did not differ between treatment groups (Supplementary Figures S10b–d).

As stable spines are considered the structural correlates of long-term memories,[41,42] we next performed the same analysis separately for persistent spines. We determined their size difference between the first and the last imaging time point (Supplementary Figure S10e). In line with our findings of higher spine turnover rates in the vicinity of plaques, we observed a significantly higher fraction of persistent spines with a large size change (difference in integrated brightness larger than the mean difference $\pm 1.5 \times$ s.d. of persistent spine-size changes in WT vehicle-treated mice) close to plaques (WT vehicle 15.4% versus APP near vehicle 27.7%, Supplementary Figure S10f). GSI treatment led to a reduction in this 'large size change fraction' of persistent spines (20.1%), which did not significantly differ anymore from WT vehicle mice (Supplementary Figure S10f).

GSI treatment did not affect spines further away from plaques and in WT mice (for data on WT mice, see Supplementary Figures S7a–d), indicating no obvious neuropathological side effect of the GSI treatment.

Owing to the high variability, it was more difficult to pinpoint the impact of the GSI on bouton dynamics (Figure 5a), but overall we found the same trend as for dendritic spines. Bouton density was not significantly affected by the GSI treatment, yet a trend towards a decrease throughout the imaging period was observed near plaques in vehicle-treated mice (Figure 5b). These findings notwithstanding, we did observe a normalization of the bouton survival fraction near plaques to levels found distant from plaques (Figure 5c). The significantly elevated bouton turnover rate near plaques was somewhat decreased by the GSI; however, the effect did not reach significance (Figure 5d). The same held true for the fraction of persistent boutons near plaques, where we observed a nonsignificant increase after the GSI treatment (one-way ANOVA, $P = 0.22$, Figure 5e).

In summary, our data demonstrate that the dynamics of both the pre- and postsynaptic compartments is affected by the amyloid plaque pathology. Moreover, we found that interference with Aβ generation by applying the GSI, ELN594, can attenuate the plaque-associated instability of synaptic structures. ELN594 does neither affect spines or boutons further away from plaques in APPPS1 nor those in WT mice, and hence seems to be devoid of apparent neuropathological side effects.

DISCUSSION

In this study, we have used a longitudinal *in vivo* two-photon imaging approach to characterize plaque-associated alterations of pre- and postsynaptic structures in a mouse model of AD. We demonstrate that interference with Aβ generation, via the application of a novel GSI, can counteract the plaque-associated synaptic instability *in vivo*.

There is growing consensus that, for a treatment against AD to be effective, it should commence already during the presymptomatic phase of the disease.[43] A number of studies performed in APP-transgenic mice have revealed an intimate relationship between amyloid plaques and structural/functional neuronal

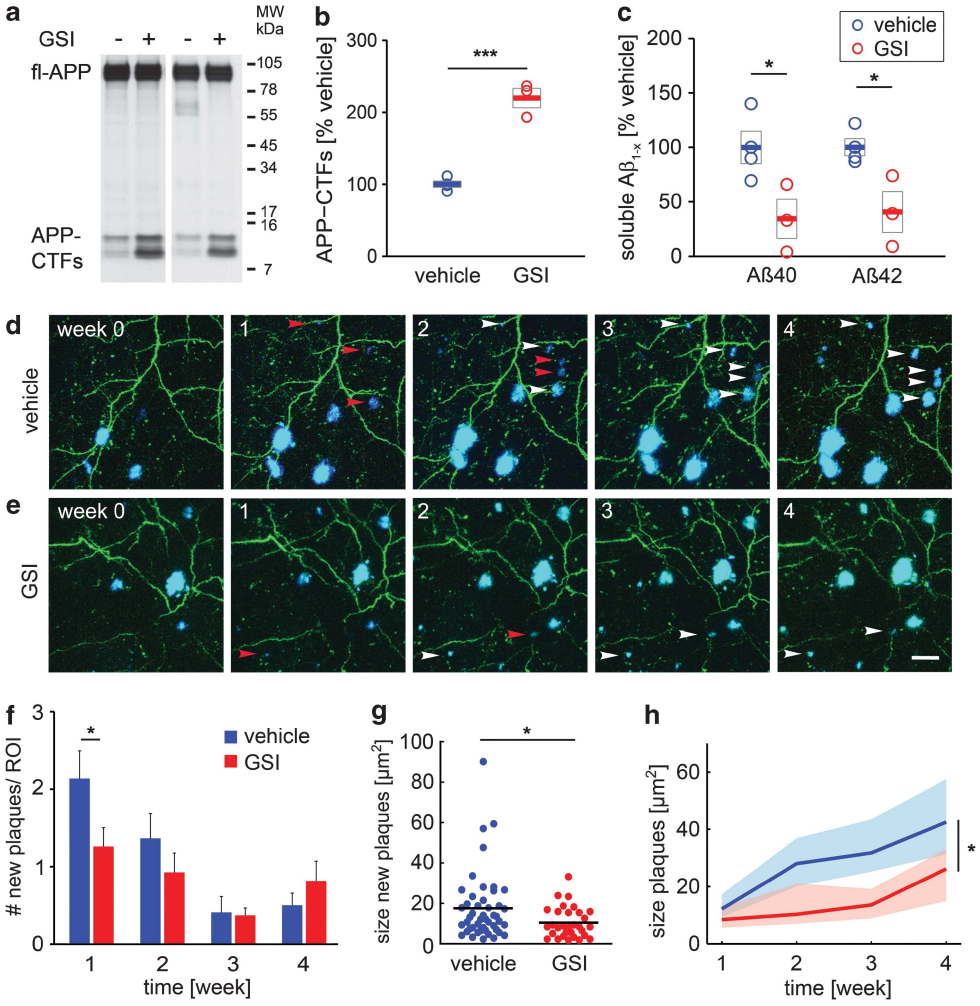

Figure 3. γ-secretase inhibitor (GSI) treatment reduces Aß generation *in vivo* and attenuates the deposition and growth of new plaques in amyloid precursor protein/presenilin 1 (APPPS1) mice. (**a**) Representative western blot analysis of the effect of GSI application on full length amyloid precursor protein (fl-APP) and APP C-terminal fragment (APP-CTF) levels in APPPS1 brain homogenates (blots of two different experiments are shown). (**b**) Quantification of GSI effect on APP-CTFs normalized to fl-APP as measured in western blot (*t*-test, $P = 0.0002$). (**c**) Quantification of ELISA analysis of soluble Aβ species (Aβ40 decreased by 66%, *t*-test, $P = 0.036$ and Aβ42 decreased by 59%, *t*-test, $P = 0.023$, vehicle $n = 4$, GSI $n = 3$ mice); open circles represent single data points, horizontal bars denote the mean and gray boxes the s.e.m. (**d** and **e**) Examples of *in vivo* two-photon images in APPPS1 mice treated daily with vehicle (**d**) and 30 mg kg^{-1} GSI (**e**), respectively. Images are maximum projections of 50 optical sections (z-spacing 5 µm) over a depth of 250 µm. Red arrowheads indicate newly formed plaques, which are marked with white arrowheads at consecutive imaging time points. (**f**) Number of newly emerged plaques per standard ROI (350 × 350 × 285 µm) are lower in GSI-treated mice after the first week: one-sided Mann–Whitney test, $P = 0.027$, values are mean ± s.e.m. (**g**) Plaques newly formed within the first week of treatment are significantly smaller in GSI-treated mice (one-sided Mann–Whitney test, $P = 0.014$); black lines denote the mean. (**h**) Newly formed plaques grow significantly slower in GSI compared with vehicle-treated mice; values are median ± 95% confidence interval of the median (repeated measures ANOVA, $P = 0.014$; APP vehicle: 22 ROIs (five mice), 45 new plaques after first week; APP GSI: 27 ROIs (seven mice), 31 new plaques after first week). Scale bar 20 µm, $^*P < 0.05$, $^{***}P < 0.001$.

alterations.[12–15,26,44] As these structural alterations are considered a precursor to eventual neuronal death, characteristic for human AD pathology,[45] mouse models are well suited to study the efficacy of candidate drugs on these early neuropathological changes.

Our results, similar to previous publications,[12,15,16] show a lower spine density and a pronounced spine instability within the immediate vicinity of amyloid plaques. The observed increase in spine turnover was attributable to almost equally enhanced spine formation and elimination rates, thereby not resulting in a change of spine density over the course of the 4-week-imaging period. Thus, the lowered spine density observed near mature plaques must result from a net spine loss at an earlier time point, probably following initial plaque formation, after which spine density stabilized again. This interpretation is supported by a recent study in an APPPS1 mouse model, which showed that plaque deposition precedes spine loss, and also found that even in aged APPPS1 mice, which already bear a substantial plaque load, spine density in the vicinity of plaques does not differ from that seen in young animals near plaques.[16]

Close to plaques, not only spine turnover was increased, but we also found that particularly persistent spines, which are thought to encode long-term memories,[41,42] varied more strongly in size over time. As spine size correlates with synapse strength,[34,38,39] this indicates that both, alterations in spine turnover as well as fluctuations in spine size, concertedly increase synaptic instability close to plaques.

Notably, despite the fact that, on average, spines distant from plaques did not behave differently from spines in WT mice, we found evidence of altered structural plasticity independent of

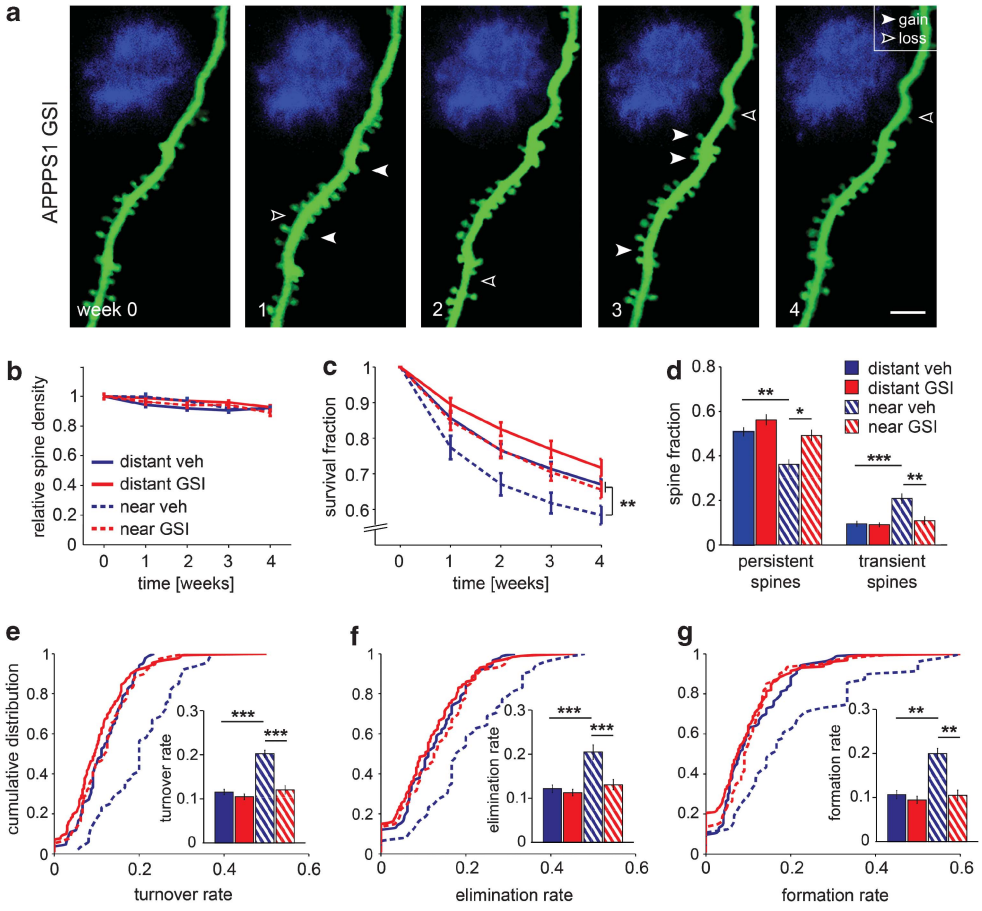

Figure 4. Effect of γ-secretase inhibitor (GSI) treatment on dendritic spines in amyloid precursor protein/presenilin 1 (APPPS1) mice. (**a**) Example of dendritic spines in a GSI-treated APPPS1 mouse in the vicinity (<50 μm) of a plaque. The first imaging session was performed prior to the start of treatment. Images are maximum projections. Open arrowheads indicate examples of spines lost between two consecutive imaging time points, filled arrowheads mark spines that were gained. (**b**) Spine density is not affected by GSI treatment in APPPS1 mice (repeated measures analysis of variance (ANOVA), $P=0.72$). (**c**) The lower survival fraction (SF) of spines in the vicinity of plaques is normalized by GSI treatment, thereby equaling the SF of spines distant from plaques in vehicle-treated mice (repeated measures ANOVA, $P<0.01$). (**d**) GSI treatment increases the fraction of persistent spines near plaques (one-way ANOVA, $P<0.05$). Accordingly, the high fraction of transient spines near plaques is reduced upon GSI treatment (one-way ANOVA, $P<0.01$). (**e**) Increased turnover of spines near plaques is reduced by the GSI (one-way ANOVA, $P<0.001$). The effect is based on normalized (**f**) elimination (one-way ANOVA, $P<0.001$) and (**g**) formation rates (Kruskal–Wallis, $P<0.01$). APP distant veh: $n=21$ dendrites (five mice); APP near veh: $n=12$ dendrites (five mice); APP distant GSI: $n=32$ dendrites (seven mice); APP near GSI: $n=15$ dendrites (seven mice). Values are mean ± s.e.m, scale bar = 5 μm, $^{*}P<0.05$, $^{**}P<0.01$, $^{***}P<0.001$.

plaque pathology. Whereas in WT mice spine density was negatively correlated with spine turnover rate, as reported previously,[30] in APPPS1 mice dendrites further away from plaques exhibited a positive correlation between spine density and turnover rate. A more detailed analysis revealed that this difference between genotypes was largely due to a reduced spine turnover on low-density stretches in APPPS1 mice. The reduction in spine dynamics on dendrites distant from plaques may indicate a weakening of synaptic efficacy. The induction of long-term potentiation (LTP) on individual spines can promote the potentiation of synapses on neighboring spines and the formation of new adjacent spines, an effect known to spread over several micrometers along the dendrite.[46–50] In APP-transgenic mice, soluble Aβ is elevated within the interstitial fluid[51] and is known to disrupt LTP induction and alter synapse composition.[52,53] This negative impact of Aβ might impede synaptic cooperativity, most prominently on dendrites bearing only a few inputs, as their combined synaptic drive, and hence the potential for 'cross-talk' between neighboring spines should be lower even under physiological conditions.

In concert with the increased turnover rate of spines near plaques, we also found that axonal boutons close to plaques were less stable. In contrast to spine density, however, bouton density did not change with plaque distance. Whereas this seems to be at odds with histological studies showing a loss of presynaptic markers close to plaques,[17–19] the latter result likely reflects the joint loss of axons (Supplementary Figure S5) and their boutons, while we measure bouton density on those axons still present close to plaques. Alternatively, the vulnerability of axonal boutons to Aβ/amyloid plaques may be cell type-specific. We have confined our analysis to intracortical axons of layer II/III/V neurons, which have a lower bouton density and are more stable compared with, for example, the axons of layer VI cells.[33]

The pathologically elevated dynamics of spines and boutons is very likely to affect synaptic plasticity, and hence memory formation, retention and retrieval, in a similar manner as the loss of synapses. Recent imaging studies have shown that the formation of long-term memories tightly correlates with the emergence of long-lived spines in the cortex.[41,42] On the other hand, inherited forms of mental retardation, such as the fragile X-syndrome, are associated with high spine turnover rates, as observed in Fmr1 (*fragile mental retardation 1*) knockout mice.[32,54] Moreover, altered dynamics of pre- and postsynaptic structures in the cortex have recently been shown to accompany normal aging

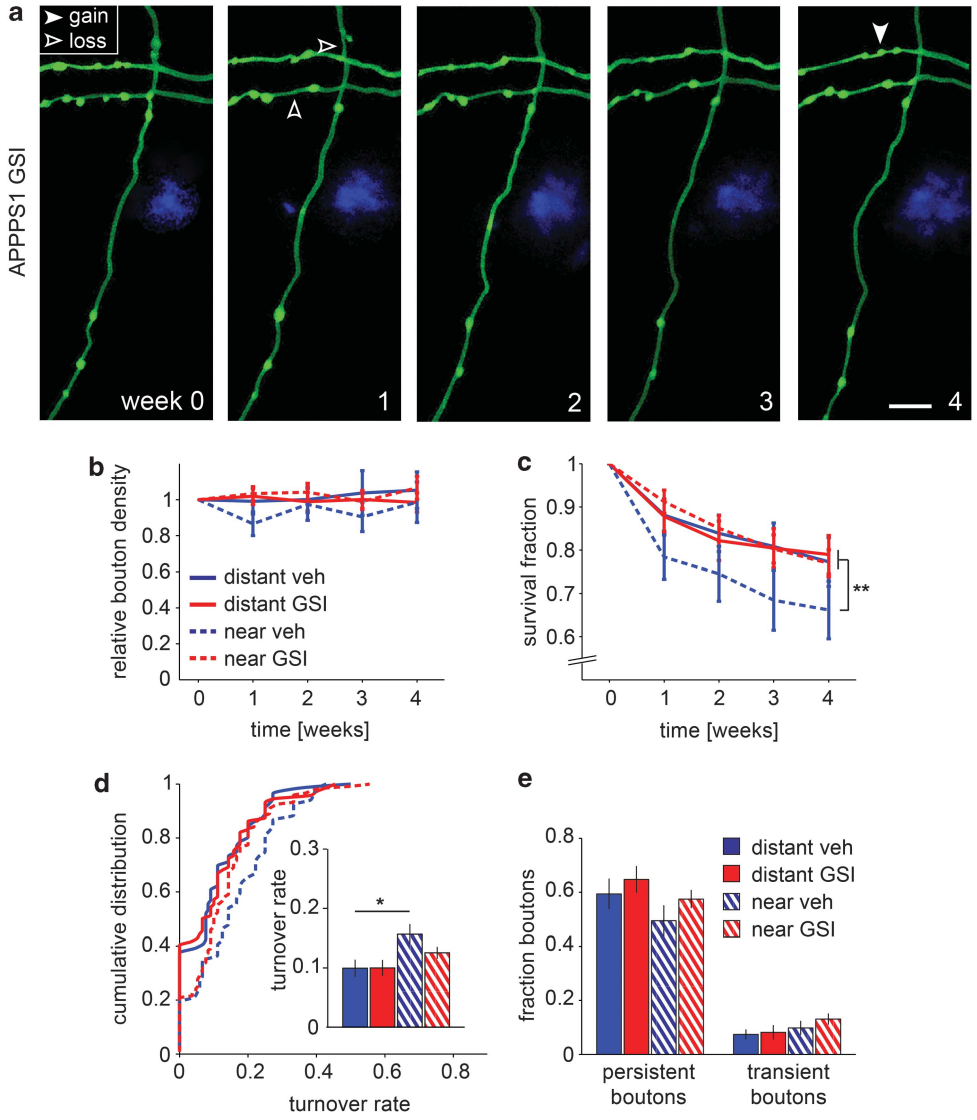

Figure 5. γ-secretase inhibitor (GSI) effect on axonal boutons in amyloid precursor protein/presenilin 1 (APPPS1) mice. (**a**) Example of an axonal stretch near a plaque in an APPPS1 mouse. (**b**) Bouton density is not affected by GSI treatment (Friedman's test, $P = 0.07$). (**c**) The lower survival fraction of boutons near plaques is normalized to levels observed distant from plaques (repeated measures analysis of variance (ANOVA), APP distant vehicle versus APP near vehicle $P < 0.01$, APP near vehicle versus APP near GSI $P < 0.001$). (**d**) The increased turnover rate of boutons near plaques is reduced after treatment; the effect did not reach significance (Kruskal–Wallis, APP near vehicle versus APP near GSI $P > 0.05$). (**e**) Bouton lifetime fractions do not differ significantly between treated and untreated mice. APP distant veh: $n = 14$ axons (four mice); APP near veh: $n = 13$ axons (four mice); APP distant GSI: $n = 18$ axons (seven mice); APP near GSI: $n = 30$ axons (seven mice). Values are means ± s.e.m., scale bar 10 μm, $^{*}P < 0.05$, $^{**}P < 0.01$.

and hence were suggested to underlie age-related cognitive deficits.[55,56] Our finding of enhanced dynamics of synaptic structures close to plaques resembles these changes observed during normal ageing, alluding to potentially similar cellular mechanisms causing the cognitive deficits during normal aging and AD. Together, these findings stress the causal relevance of altered spine and bouton dynamics for neurodegenerative diseases and, furthermore, imply that the impact of synaptic instability on the cognitive decline seen in AD might have been underestimated thus far.

The molecular mechanisms underlying the enhanced turnover of synaptic structures close to plaques are not well understood. Plaques are considered a reservoir of soluble Aβ that seems to extend with a gradient beyond the histological border of the dense core plaque.[6,10,12] This locally elevated concentration of soluble Aβ in the plaque region might cause the structural and functional alterations predominantly seen in the vicinity of plaques, such as dysmorphic neurites,[26] changes in spine stability and spine density,[12,15,16] as well as the occurrence of clusters of hyperactive cells and Ca^{2+}-overloaded dendrites.[27,44] Spines on Ca^{2+}-overloaded dendrites lack functional compartmentalization,[27] a property considered a prerequisite for synaptic integration.[57,58] The breakdown of spine compartmentalization in a subset of dendrites near plaques might account for the observed spine instability.

In addition to plaques, other pathological events associated with AD also affect synaptic structures. A recent *in vivo* imaging study performed in triple transgenic AD mice (bearing in addition to the APPswe and $PS1_{M146V}$ also the Tau_{P301L} mutation[59]) suggests that intraneuronal hyperphosphorylated tau can have a strong impact on spine density as well.[60] The authors describe spine loss on dystrophic dendrites positive for hyperphosphorylated tau in brain areas that were devoid of plaques.

Furthermore, in areas with substantial plaque load, spine density was found to be lower even distant from plaques ($>50\,\mu m$).[60]

Having found that amyloid plaques cause local synaptic instability, we next tested whether Aβ-targeting treatment can exert beneficial effects on this pathology. At the concentration used, the GSI, ELN594, inhibited γ-secretase effectively, reducing Aβ generation in APPPS1 mice to levels comparable to those observed with other GSIs in different APP-transgenic mice.[22,61,62] We found that the lowered Aβ levels caused an initial attenuation of new plaque deposition and a sustained diminished growth of the newly formed plaques throughout the treatment period, in line with a previous report showing that GSI treatment can suppress the formation of new plaques.[21] The observed overall decline in the number of newly formed plaques in the treatment *and* control group might reflect the age dependency of *de novo* plaque formation[63] or could be attributable to the anti-amyloidogenic properties of Methoxy-XO4,[64] which we applied repeatedly in order to label plaques *in vivo*. However, both the vehicle- and the GSI-treated groups should be affected equally by Methoxy-XO4, thus essentially resulting in a potential underestimation of the GSI effect on plaque formation.

The moderate GSI effect on plaque pathology was accompanied by a substantial impact on synaptic structures in the vicinity of plaques. GSI treatment specifically reduced the plaque-associated spine instability, resulting in spine turnover rates comparable to those found in regions distal to plaques. Similarly, the GSI reduced the increased size fluctuations of persistent spines close to plaques. Intriguingly, a more detailed analysis of the 'near plaque' spine cohort ($<50\,\mu m$ away) revealed that GSI treatment normalized, in particular, the dynamics of spines located $>15\,\mu m$ away from the plaque border. As soluble Aβ levels gradually fall off next to dense core plaques,[10] we propose that the synapse-stabilizing effect of ELN594 occurs in a threshold-dependent manner. We assume that the lower concentrations of Aβ at the periphery of the plaque-surrounding halo is cleared more rapidly once additional Aβ generation is inhibited via the GSI, and as a consequence synaptic structures located there recover from elevated turnover more readily than those still in tight contact with the dense core plaque and higher Aβ levels.

In a recent two-photon imaging study, GSI treatment was shown to restore the pathologically enhanced neuronal-activity levels in hippocampal CA1 neurons in predepositing APP-transgenic mice.[65] In depositing mice, however, hyperactive cells are exclusively found within the vicinity of plaques both in the hippocampus and the cortex.[44,65] It remains to be clarified whether GSI treatment in depositing mice can prevent this neuronal dysfunction in an equally effective manner as observed in predepositing mice,[65] which then would suggest a link between our finding of GSI-induced synapse stabilization and the normalization of neuronal-activity patterns near plaques.

We did not observe any effect of the GSI on dendrites distant from plaques in APPPS1 mice nor on spines in WT mice. This is at odds with a recently published study, which reported a GSI-induced rapid and prolonged decrease in spine density in WT mice after a short treatment period of 4 days.[37] Earlier-generation GSIs are known to non-selectively interfere with the processing of other γ-secretase substrates. In particular, impaired cleavage of Notch, a cell-surface receptor involved in cell differentiation and development,[66] is thought to cause side effects of GSI treatment. The inhibitors used in the above mentioned study, DAPT and LY450139 (semagacestat), are unselective GSIs (ratio of EC_{50} values for Notch and Aβ42: DAPT = 0.5; LY450139 = 0.8[67]) and belong to a different structural class than the second-generation compound ELN594, a sulfonamide-type GSI with an at least 10-fold higher selectivity of APP over Notch substrate cleavage (data not shown). The previously investigated compounds might also substantially differ in their pharmacokinetic and pharmacologic properties, factors, which may further contribute to a different side effect profile. It is also conceivable that the compounds used in the previous study might have had off-target effects. Chronic administration of ELN594 on the other hand did not affect dendritic spines or axonal boutons in WT mice or APPPS1 mice distant from plaques and hence seems to be devoid of those aforementioned side effects.

Taken together, we here for the first time demonstrate *in vivo* the ability of a GSI to selectively alleviate plaque-associated synaptic pathology in a mouse model of AD. Given that the impact of plaques on the density of spines has been shown in various brain regions, such as neocortex and hippocampus,[12,14–16] we believe that the plaque-associated enhanced dynamics of synaptic structures represents a general mechanism by which plaques convey their detrimental effects on synapses. Thus, the GSI effect on synapses should pertain to other brain regions as well. Our data, moreover, argue in favor of the amyloid cascade hypothesis and serve as a proof of principle regarding the efficacy of pharmacological interference with Aβ generation.

CONFLICT OF INTEREST

KQ, EG, EFB, DQ, GSB, DBS either were, or currently still are, employees of Elan Pharmaceuticals. at the time the studies reported in this manuscript were being conducted, hold (or held) stock in Elan and are inventors on patent filings resulting from the work described herein. CH has acted as a consultant for Elan Pharmaceuticals. All other authors declare no conflict of interests.

ACKNOWLEDGMENTS

We would like to thank Victoria Milde, Claudia Abou-Ajram and Claudia Huber for their help with data analysis and technical assistance. We also thank Mathias Jucker for providing the APPPS1 mice. This work was supported by the Emmy Noether Program of the DFG (MM-L), the SFB 596 'Molecular Mechanisms of Neurodegeneration' of the DFG (CH, HS), the European Research Council under the European Union's Seventh Framework Programme (FP7/2007–2013)/ERC Grant Agreement No. 321366-Amyloid (advanced grant to CH), the KNDD of the BMBF (CH, HS), the Center for Integrated Protein Science Munich, Hans and Ilse Breuer Foundation (MM-L), the Graduate School of Systemic Neurosciences (SL), the International Max Planck Research School (SL) and the Max Planck Society (SL, TB, MH). CH is supported by a research professorship by the LMUexcellent program.

REFERENCES

1 Masliah E, Terry RD, Alford M, DeTeresa R, Hansen LA. Cortical and subcortical patterns of synaptophysinlike immunoreactivity in Alzheimer's disease. *Am J Pathol* 1991; **138**: 235–246.
2 Terry RD *et al.* Physical basis of cognitive alterations in Alzheimer's disease: synapse loss is the major correlate of cognitive impairment. *Ann Neurol* 1991; **30**: 572–580.
3 Scheff SW, Price DA. Alzheimer's disease-related alterations in synaptic density: neocortex and hippocampus. *J Alzheimers Dis* 2006; **9**(3 Suppl): 101–115.
4 Koffie RM, Hyman BT, Spires-Jones TL. Alzheimer's disease: synapses gone cold. *Mol Neurodegener* 2011; **6**: 63.
5 Selkoe DJ. Alzheimer's disease is a synaptic failure. *Science* 2002; **298**: 789–791.
6 Haass C, Selkoe DJ. Soluble protein oligomers in neurodegeneration: lessons from the Alzheimer's amyloid beta-peptide. *Nat Rev Mol Cell Biol* 2007; **8**: 101–112.
7 Wu HY *et al.* Amyloid beta induces the morphological neurodegenerative triad of spine loss, dendritic simplification, and neuritic dystrophies through calcineurin activation. *J Neurosci* 2010; **30**: 2636–2649.
8 Lacor PN *et al.* Abeta oligomer-induced aberrations in synapse composition, shape, and density provide a molecular basis for loss of connectivity in Alzheimer's disease. *J Neurosci* 2007; **27**: 796–807.
9 Cisse M *et al.* Reversing EphB2 depletion rescues cognitive functions in Alzheimer model. *Nature* 2011; **469**: 47–52.
10 Koffie RM *et al.* Oligomeric amyloid beta associates with postsynaptic densities and correlates with excitatory synapse loss near senile plaques. *Proc Natl Acad Sci USA* 2009; **106**: 4012–4017.
11 Spires-Jones T, Knafo S. Spines, plasticity, and cognition in Alzheimer's model mice. *Neural Plast* 2012; **2012**: 319836.
12 Spires-Jones TL *et al.* Impaired spine stability underlies plaque-related spine loss in an Alzheimer's disease mouse model. *Am J Pathol* 2007; **171**: 1304–1311.

13 Spires TL *et al.* Dendritic spine abnormalities in amyloid precursor protein transgenic mice demonstrated by gene transfer and intravital multiphoton microscopy. *J Neurosci* 2005; **25**: 7278–7287.
14 Grutzendler J, Helmin K, Tsai J, Gan WB. Various dendritic abnormalities are associated with fibrillar amyloid deposits in Alzheimer's disease. *Ann N Y Acad Sci* 2007; **1097**: 30–39.
15 Tsai J, Grutzendler J, Duff K, Gan WB. Fibrillar amyloid deposition leads to local synaptic abnormalities and breakage of neuronal branches. *Nat Neurosci* 2004; **7**: 1181–1183.
16 Bittner T *et al.* Amyloid plaque formation precedes dendritic spine loss. *Acta Neuropathol* 2012; **124**: 797–807.
17 King DL, Arendash GW. Maintained synaptophysin immunoreactivity in Tg2576 transgenic mice during aging: correlations with cognitive impairment. *Brain Res* 2002; **926**: 58–68.
18 Boncristiano S *et al.* Neocortical synaptic bouton number is maintained despite robust amyloid deposition in APP23 transgenic mice. *Neurobiol Aging* 2005; **26**: 607–613.
19 Dong H, Martin MV, Chambers S, Csernansky JG. Spatial relationship between synapse loss and beta-amyloid deposition in Tg2576 mice. *J Comp Neurol* 2007; **500**: 311–321.
20 Steiner H, Fluhrer R, Haass C. Intramembrane proteolysis by gamma-secretase. *J Biol Chem* 2008; **283**: 29627–29631.
21 Yan P *et al.* Characterizing the appearance and growth of amyloid plaques in APP/PS1 mice. *J Neurosci* 2009; **29**: 10706–10714.
22 Best JD *et al.* The novel gamma secretase inhibitor N-[cis-4-[(4-chlorophenyl)sulfonyl]-4-(2,5-difluorophenyl)cyclohexyl]-1,1, 1-trifluoromethanesulfonamide (MRK-560) reduces amyloid plaque deposition without evidence of notch-related pathology in the Tg2576 mouse. *J Pharmacol Exp Ther* 2007; **320**: 552–558.
23 Radde R *et al.* Abeta42-driven cerebral amyloidosis in transgenic mice reveals early and robust pathology. *EMBO Rep* 2006; **7**: 940–946.
24 Feng G *et al.* Imaging neuronal subsets in transgenic mice expressing multiple spectral variants of GFP. *Neuron* 2000; **28**: 41–51.
25 Truong AP *et al.* Design, synthesis, and structure-activity relationship of novel orally efficacious pyrazole/sulfonamide based dihydroquinoline gamma-secretase inhibitors. *Bioorg Med Chem Lett* 2009; **19**: 4920–4923.
26 Meyer-Luehmann M *et al.* Rapid appearance and local toxicity of amyloid-beta plaques in a mouse model of Alzheimer's disease. *Nature* 2008; **451**: 720–724.
27 Kuchibhotla KV, Goldman ST, Lattarulo CR, Wu HY, Hyman BT, Bacskai BJ. Abeta plaques lead to aberrant regulation of calcium homeostasis *in vivo* resulting in structural and functional disruption of neuronal networks. *Neuron* 2008; **59**: 214–225.
28 Liebscher S, Meyer-Luehmann MA. Peephole into the brain: neuropathological features of Alzheimer's disease revealed by *in vivo* two-photon imaging. *Front Psychiatry* 2012; **3**: 26.
29 Trachtenberg JT *et al.* Long-term *in vivo* imaging of experience-dependent synaptic plasticity in adult cortex. *Nature* 2002; **420**: 788–794.
30 Holtmaat AJ *et al.* Transient and persistent dendritic spines in the neocortex *in vivo*. *Neuron* 2005; **45**: 279–291.
31 Hofer SB, Mrsic-Flogel TD, Bonhoeffer T, Hübener M. Experience leaves a lasting structural trace in cortical circuits. *Nature* 2009; **457**: 313–317.
32 Pan F, Aldridge GM, Greenough WT, Gan WB. Dendritic spine instability and insensitivity to modulation by sensory experience in a mouse model of fragile X syndrome. *Proc Natl Acad Sci USA* 2010; **107**: 17768–17773.
33 De Paola V *et al.* Cell type-specific structural plasticity of axonal branches and boutons in the adult neocortex. *Neuron* 2006; **49**: 861–875.
34 Knott GW, Holtmaat A, Wilbrecht L, Welker E, Svoboda K. Spine growth precedes synapse formation in the adult neocortex *in vivo*. *Nat Neurosci* 2006; **9**: 1117–1124.
35 Moehlmann T *et al.* Presenilin-1 mutations of leucine 166 equally affect the generation of the Notch and APP intracellular domains independent of their effect on Abeta 42 production. *Proc Natl Acad Sci USA* 2002; **99**: 8025–8030.
36 Czirr E *et al.* Insensitivity to Abeta42-lowering nonsteroidal anti-inflammatory drugs and gamma-secretase inhibitors is common among aggressive presenilin-1 mutations. *J Biol Chem* 2007; **282**: 24504–24513.
37 Bittner T *et al.* Gamma-secretase inhibition reduces spine density *in vivo* via an amyloid precursor protein-dependent pathway. *J Neurosci* 2009; **29**: 10405–10409.
38 Harris KM, Stevens JK. Dendritic spines of CA 1 pyramidal cells in the rat hippocampus: serial electron microscopy with reference to their biophysical characteristics. *J Neurosci* 1989; **9**: 2982–2997.
39 Kasai H, Fukuda M, Watanabe S, Hayashi-Takagi A, Noguchi J. Structural dynamics of dendritic spines in memory and cognition. *Trends Neurosci* 2010; **33**: 121–129.
40 Loewenstein Y, Kuras A, Rumpel S. Multiplicative dynamics underlie the emergence of the log-normal distribution of spine sizes in the neocortex *in vivo*. *J Neurosci* 2011; **31**: 9481–9488.
41 Xu T *et al.* Rapid formation and selective stabilization of synapses for enduring motor memories. *Nature* 2009; **462**: 915–919.
42 Yang G, Pan F, Gan WB. Stably maintained dendritic spines are associated with lifelong memories. *Nature* 2009; **462**: 920–924.
43 Gandy S, Dekosky ST. 2012: the year in dementia. *Lancet Neurol* 2013; **12**: 4–6.
44 Busche MA *et al.* Clusters of hyperactive neurons near amyloid plaques in a mouse model of Alzheimer's disease. *Science* 2008; **321**: 1686–1689.
45 Coleman P, Federoff H, Kurlan R. A focus on the synapse for neuroprotection in Alzheimer disease and other dementias. *Neurology* 2004; **63**: 1155–1162.
46 Engert F, Bonhoeffer T. Dendritic spine changes associated with hippocampal long-term synaptic plasticity. *Nature* 1999; **399**: 66–70.
47 Yuste R, Bonhoeffer T. Morphological changes in dendritic spines associated with long-term synaptic plasticity. *Annu Rev Neurosci* 2001; **24**: 1071–1089.
48 Harvey CD, Svoboda K. Locally dynamic synaptic learning rules in pyramidal neuron dendrites. *Nature* 2007; **450**: 1195–1200.
49 De Roo M, Klauser P, Muller D. LTP promotes a selective long-term stabilization and clustering of dendritic spines. *PLoS Biol* 2008; **6**: e219.
50 Harnett MT, Makara JK, Spruston N, Kath WL, Magee JC. Synaptic amplification by dendritic spines enhances input cooperativity. *Nature* 2012; **491**: 599–602.
51 Hong S *et al.* Dynamic analysis of amyloid beta-protein in behaving mice reveals opposing changes in ISF versus parenchymal Abeta during age-related plaque formation. *J Neurosci* 2011; **31**: 15861–15869.
52 Shankar GM *et al.* Amyloid-beta protein dimers isolated directly from Alzheimer's brains impair synaptic plasticity and memory. *Nat Med* 2008; **14**: 837–842.
53 Selkoe DJ. Soluble oligomers of the amyloid beta-protein impair synaptic plasticity and behavior. *Behav Brain Res* 2008; **192**: 106–113.
54 Cruz-Martin A, Crespo M, Portera-Cailliau C. Delayed stabilization of dendritic spines in fragile X mice. *J Neurosci* 2010; **30**: 7793–7803.
55 Grillo FW *et al.* Increased axonal bouton dynamics in the aging mouse cortex. *Proc Natl Acad Sci USA* 2013; **110**: E1514–E1523.
56 Mostany R, Anstey JE, Crump KL, Maco B, Knott G, Portera-Cailliau C. Altered synaptic dynamics during normal brain aging. *J Neurosci* 2013; **33**: 4094–4104.
57 Grunditz A, Holbro N, Tian L, Zuo Y, Oertner TG. Spine neck plasticity controls postsynaptic calcium signals through electrical compartmentalization. *J Neurosci* 2008; **28**: 13457–13466.
58 Araya R, Eisenthal KB, Yuste R. Dendritic spines linearize the summation of excitatory potentials. *Proc Natl Acad Sci USA* 2006; **103**: 18799–18804.
59 Oddo S *et al.* Triple-transgenic model of Alzheimer's disease with plaques and tangles: intracellular Abeta and synaptic dysfunction. *Neuron* 2003; **39**: 409–421.
60 Bittner T *et al.* Multiple events lead to dendritic spine loss in triple transgenic Alzheimer's disease mice. *PLoS One* 2010; **5**: e15477.
61 Lanz TA *et al.* The gamma-secretase inhibitor N-[N-(3,5-difluorophenacetyl)-L-alanyl]-S-phenylglycine t-butyl ester reduces A beta levels *in vivo* in plasma and cerebrospinal fluid in young (plaque-free) and aged (plaque-bearing) Tg2576 mice. *J Pharmacol Exp Ther* 2003; **305**: 864–871.
62 Abramowski D *et al.* Dynamics of Abeta turnover and deposition in different beta-amyloid precursor protein transgenic mouse models following gamma-secretase inhibition. *J Pharmacol Exp Ther* 2008; **327**: 411–424.
63 Hefendehl JK *et al.* Long-term *in vivo* imaging of beta-amyloid plaque appearance and growth in a mouse model of cerebral beta-amyloidosis. *J Neurosci* 2011; **31**: 624–629.
64 Cohen AD *et al.* Anti-amyloid effects of small molecule abeta-binding agents in PS1/APP Mice. *Lett Drug Des Discov* 2009; **6**: 437.
65 Busche MA *et al.* Critical role of soluble amyloid-beta for early hippocampal hyperactivity in a mouse model of Alzheimer's disease. *Proc Natl Acad Sci USA* 2012; **109**: 8740–8745.
66 Ables JL, Breunig JJ, Eisch AJ, Rakic P. Not(ch) just development: Notch signalling in the adult brain. *Nat Rev Neurosci* 2011; **12**: 269–283.
67 Martone RL *et al.* Begacestat (GSI-953): a novel, selective thiophene sulfonamide inhibitor of amyloid precursor protein gamma-secretase for the treatment of Alzheimer's disease. *J Pharmacol Exp Ther* 2009; **331**: 598–608.

Supplementary Information accompanies the paper on the Molecular Psychiatry website (http://www.nature.com/mp)